Cambrian magmatic activization of the East European craton

ARTICLE *in* DOKLADY EARTH SCIENCES · AUGUST 2015

Impact Factor: 0.5

4 AUTHORS, INCLUDING:

Savko Konstantin
Voronezh State University

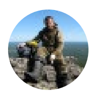

Roman Terentiev
Voronezh State University

ISSN 1028-334X, Doklady Earth Sciences, 2015, Vol. 463, Part 2, pp. 822–827. © Pleiades Publishing, Ltd., 2015.
Original Russian Text © V.Yu. Skryabin, K.A. Savko, M.V. Skryabin, R.A. Terentiev, 2015, published in Doklady Akademii Nauk, 2015, Vol. 463, No. 5, pp. 581–586.

GEOCHEMISTRY

Cambrian Magmatic Activation of the East European Platform

V. Yu. Skryabin†, K. A. Savko, M. V. Skryabin, and R. A. Terentiev

Presented by Academician Yu.M. Pushcharovskii December 5, 2013

Received December 19, 2013

DOI: 10.1134/S1028334X15080140

The East European Platform (EEP), since assembly of its constitutent landmasses in the Paleoproterozoic, has undergone repeated magmatic activation in the Mesozoic, Neoproterozoic, and Phanerozoic. The youngest manifestations of the Neoproterozoic (Vendian) within-plate magmatism are represented by alkali volcanic rocks and their tuffs in the Belomorian rift system (570 ± 8 to 555.3 ± 0.3 Ma) [7, 9] as well as basalts and tuffs of the Volhyn–Brest flood-basalt province (551 ± 4 Ma) [8]. Subsequent magmatic activation of the EEP occurred as late as the Devonian and resulted in the formation of basalts in the eastern part of the Voronezh crystalline massif [2], dolerite dikes (389 ± 4 to 355 ± 10 Ma) [1, 10] and alkaline rocks (380–360 Ma) [4] in the Baltic shield, and kimberlites in the White Sea region (360–340 Ma) [3, 5]. From the Upper Vendian to the Devonian time, no magmatic activity is known yet in the EEP.

The examination of new geochemical and zircon U–Pb data allowed us to reveal for the first time the Cambrian stage of the magmatic activation of the EEP, which is manifested by the emplacement of subvolcanic syenite dikes distinguished as the Artyushki Complex in the northeastern part of the Voronezh crystalline massif.

This dike complex is recovered by boreholes within four sites forming a 75-km long chain parallel to the southwestern wall of the Pachelma aulacogen. Within the Artyushki site, the best studied by boreholes, the dikes form a group of closely spaced bodies with a general strike around 300° NW and dip at 20°–60° to the northeast. The thickness of the dike bodies varies from 0.1 to 34.2 m. One hundred twenty-four dikes were recovered from 2156.8 m of the total borehole section; they occupy 3–35% of the section, averaging 22%. At the contact with dikes, host Paleoproterozoic metaterrigenous rocks of the Vorontsovka Group were hornfelsed and fenitized.

The dike rocks vary in color from gray and greenish gray to pink and red-brown and usually have a porphyritic texture with phenocrysts of feldspar and mafic minerals embedded in a fine-grained groundmass. K–Na feldspar phenocrysts up to 2 cm in size are characterized by a gradual increase in the potassium content from the core (hereinafter, in mol %, $Ab_{75.3-81.4}An_{9.4-15.3}Or_{6.2-10.3}$) to the intermediate growth zones ($Ab_{50.6-72.9}Or_{19.1-47.3}An_{2.2-8.9}$) and crystal margin ($Or_{69.5-79.1}Ab_{20.9-30.5}An_{0.0}$). The phenocrysts of mafic minerals are represented by zoned augite–aegirine-augite with an increase in the acmite end member to their rims ($Aug_{80.8-83.2}Ac_{6.5-15.0}Jd_{4.2-10.3}$) and by garnet (melanite, TiO_2 3.53–3.18 wt %) showing an anomalous birefringence with scarce thin concentric zoning and mainly grossular–andradite composition ($And_{53.5-60.6}Grs_{28.1-31.3}Alm_{5.1-7.7}Sps_{3.2-3.6}$). The groundmass of syenite porphyries is made up of fine-grained sanidine aggregate ($Or_{85.8-95.3}Ab_{4.7-14.2}An_{0.0-1.5}$) and albite ($Ab_{93.4-100.0}An_{0.0-4.8}Or_{0.0-4.1}$) with aegirine needles ($Ac_{73.5-89.4}Aug_{8.7-26.5}Jd_{0.0-5.8}$) and biotite flakes. Fine garnet grains in the groundmass are characterized by a lower TiO_2 (1.68–0.90 wt %) and a higher content of the grossular component ($And_{52.5-57.4}Grs_{40.0-41.6}Sps_{2.6-6.6}Alm_{0.0}$) as compared to the melanite phenocrysts.

Chemically, the dike rocks vary from alkali syenite to syenite and quartz syenite of K–Na to K and the ultra-K series (Table 1). Statistically significant (probability > 0.95, t_r = 6.544–2.258 at $q_{0.05}$ = 2.101) relations of indicator ratios K/Ba (r = 0.839) and Ba/Rb (r = –0.470) with the K/Na ratio indicate that potassic and ultrapotassic rock varieties could not be formed through crystallization differentiation. The associated increase in the Cl content from 0.015% in the K–Na rocks to 0.024% in the K and ultra-K varieties suggest their formation by postmagmatic cation–exchange substitution $K^+ \rightarrow Na^+$ and $2K^+ \rightarrow Ca^{2+}$ under the effect of KCl solutions on the primary syenites [6]. Variations of SiO_2 contents in the dike rocks are prob-

† Deceased.

Voronezh State University, Voronezh, Russia
e-mail: terentiev@geol.vsu.ru

Table 1. Chemical composition of subvolcanic dike rocks of the Artyushki Complex (wt %)

Components	Alkali syenite ($n = 24$)	K–Na syenite ($n = 24$)	Quartz syenite ($n = 3$)	K syenite ($n = 23$)	Ultra-K syenite ($n = 14$)
SiO_2	59.32	60.60	65.36	58.79	58.82
TiO_2	0.37	0.46	0.34	0.37	0.22
Al_2O_3	19.04	18.43	15.50	18.62	18.44
Fe_2O_3	1.56	1.74	1.60	1.74	1.52
FeO	2.06	2.15	2.99	1.76	1.60
MnO	0.10	0.08	0.09	0.07	0.09
MgO	0.69	0.97	0.99	0.73	0.51
CaO	2.72	2.62	2.11	2.29	1.47
Na_2O	7.29	5.63	4.35	3.96	0.66
K_2O	4.51	4.95	5.21	8.45	14.15
P_2O_5	0.13	0.13	0.13	0.12	0.07
L.O.I.	1.86	1.59	1.54	2.26	1.18
Total	99.65	99.35	100.21	99.16	98.73

ably caused by assimilation of host quartz–plagioclase silty sandstones of the Vorontsovska Group by primary syenite magma, which is confirmed by the distribution of different genetic types of zircons in them.

In all rock varieties, zircon occurs as syngenetic grains and xenocrystals, which differ in their inner structure, morphology, and geochemistry. Most zircons in the primary alkali syenites are ascribed to the syngenetic type, whereas contaminated (SiO_2-saturated and oversaturated) syenite varieties contain mainly xenocrysts.

Syngenetic zircons are euhedral, fine, 0.066–0.108 mm long and 0.057–0.074 mm wide, equant or weakly elongated (l/m 1.1—1.7) prismatic transparent crystals with a pale brownish tint. They show weak cathodoluminescence in dark gray tones and a homogenous inner structure (Fig. 1a). Zircon xenocrysts, unlike syngenetic grains, have brighter cathodoluminescence and thin concentric (oscillatory) zoning. In most cases, the grains are represented by fragments, the boundaries of which cut across growth zoning and are covered by regeneration rims (Fig. 1b) up to 0.051 mm thick. Xenocrysts differ statistically (probability > 0.95) from syngetic grains in the lower U and Th contents and Th/U ratio (Student test t 2.123–3.313; $t_{0.05} = 2.101$), and lower dispersion (Fisher test $F = 12–11766$, $F_{0.05} = 3.00$) of these values. The regeneration rims on the xenocrysts are similar to the syngenetic grains in terms of the inner structure and cathodoluminescence intensity. The U and Pb isotope ratios in them, however, vary within the entire observed range for different genetic types of zircon from concordant values of syngenetic grains to concordant values of xenocrysts.

The results of isotope studies (Table 2, Fig. 2) indicate the absence or insignificant disturbance of the U–Pb isotope system in syngenetic zircons and Cambrian values of their concordant age both in the primary alkali syenite porphyries (523.3 ± 2.6 Ma) and in the contaminated and metasomatically altered potassic and ultrapotassic varieties (517 ± 11 Ma). The calculated concordant ages of syngenetic grains are consistent with the lower discordia intercepts (524.2 ± 4.7 and 527 ± 81 Ma, respectively) for zircons from all types of dike rocks. The concordant age of xenogenic zircons entrapped from host rocks varies from the oldest 2200 ± 26 Ma found in one grain to 2143 ± 14 Ma for most xenocrysts from contaminated syenite porphyries. The concordant isotope dates obtained for most of xenogenic zircons are consistent with the upper intercept (2135 ± 12 Ma) and correspond to the Paleoproterozoic age.

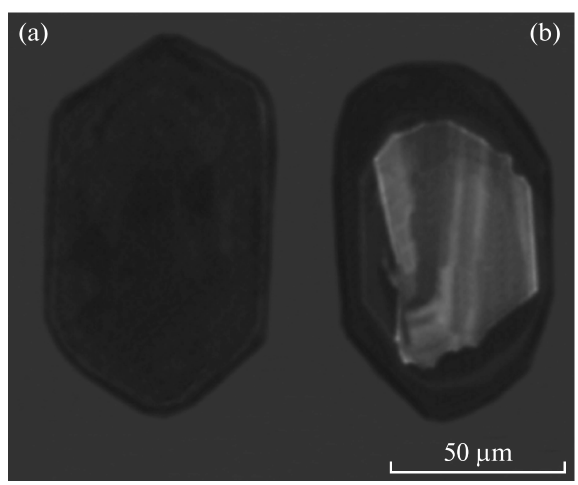

Fig. 1. Types of zircons in the subvolcanic dike syenite porphyries of the Artyushki Complex. (a) Syngenetic crystal, (b) detrital xenocryst with regeneration rim.

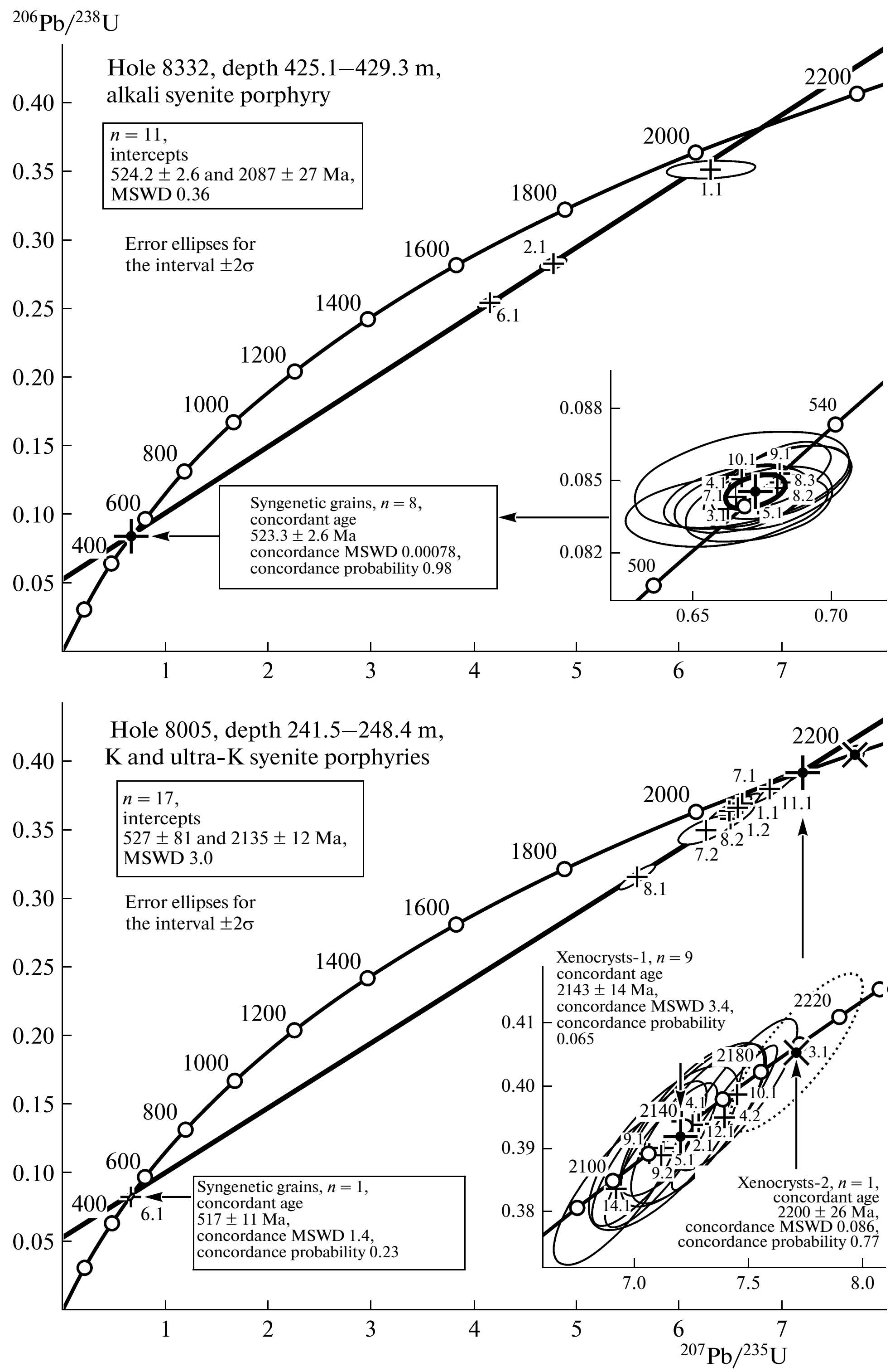

Fig. 2. Isotope U–Pb ratios in zircons from subvolcanic dike syenite porphyries of the Artyushki Complex. The numbers of analytical points correspond to those presented in Table 2.

Thus, the results of geochemical and isotope-geochemical studies of different genetic types of zircons indicate the manifestation of the Cambrian (523.3 ± 2.6 Ma) magmatic activation in the East European Platform. This activation within the northeastern part of the Voronezh crystalline massif produced a subvolcanic dike complex by the emplacement of the initial alkali syenite magma, its contami-

Table 2. Contents and isotope ratios of Pb, U, and Th in zircons from subvolcanic dike syenite porphyries of the Artyushki Complex

Ordinal no.	Grain no., analysis spot	$^{206}Pb_c$, %	U, ppm	Th, ppm	$^{232}Th/^{238}U$	$^{206}Pb^*$, ppm	(1) Age $^{206}Pb/^{238}U$ Ma	±, σ	(1) Age $^{207}Pb/^{206}Pb$ Ma	±, σ	*D*, %	(1) $^{207}Pb^*/^{206}Pb^*$	±, %	(1) $^{207}Pb^*/^{235}U$	±, %	(1) $^{206}Pb^*/^{238}U$	±, %	Error corr.
Hole 8332, depth 425.1–429.3 m; alkali syenite porphyry																		
Syngenetic grains																		
1	9.1	0.41	1859	458	0.25	137	528	3	528	21	0	0.0580	1.0	0.682	1.1	0.0853	0.6	0.544
2	10.1	0.15	724	277	0.40	53	522	3	510	29	–2	0.0575	1.3	0.668	1.5	0.0843	0.7	0.450
3	3.1	0.31	558	26228	48.61	40	519	4	505	49	–3	0.0574	2.2	0.663	2.3	0.0839	0.7	0.313
4	5.1	0.06	371	19635	54.64	27	520	4	536	31	3	0.0582	1.4	0.674	1.6	0.0841	0.8	0.470
5	7.1	0.13	1027	562	0.57	75	522	3	501	32	–4	0.0573	1.4	0.666	1.6	0.0844	0.7	0.412
6	4.1	0.00	142	28	0.20	10	526	5	489	49	–7	0.0569	2.2	0.668	2.4	0.0851	1.0	0.403
Regeneration rim around xenocryst																		
7	8.3	0.00	386	145	0.39	28	526	4	539	29	3	0.0583	1.3	0.682	1.5	0.0850	0.7	0.490
8	8.2	0.00	341	101	0.31	25	524	4	542	30	3	0.0583	1.4	0.681	1.6	0.0847	0.9	0.523
Xenocrysts with disturbed U–Pb isotope system																		
9	1.1	0.08	248	151	0.63	75	1943	12	2098	48	8	0.1300	2.7	6.310	2.8	0.3517	0.7	0.262
10	2.1	0.32	446	324	0.75	109	1608	10	1992	16	29	0.1224	0.9	4.780	1.1	0.2832	0.7	0.586
11	6.1	0.43	577	178	0.32	127	1462	9	1934	16	32	0.1185	0.9	4.161	1.1	0.2546	0.7	0.597
Hole 8005, depth 241.5–284.4 m, K and ultra-K syenite porphyry																		
Syngenetic grains																		
12	6.1	0.08	1545	814	0.54	110	515	6	546	25	6	0.0584	1.2	0.670	1.7	0.0832	1.2	0.714

Table 2. (Contd.)

Ordinal no.	Grain no., analysis spot	$^{206}Pb_c$, %	U, ppm	Th, ppm	$^{232}Th/^{238}U$	$^{206}Pb^*$, ppm	(1) Age $^{206}Pb/^{238}U$ Ma	±, σ	(1) Age $^{207}Pb/^{206}Pb$ Ma	±, σ	*D*, %	(1) $^{207}Pb^*/^{206}Pb^*$	±, %	(1) $^{207}Pb^*/^{235}U$	±, %	(1) $^{206}Pb^*/^{238}U$	±, %	Error corr.
Regeneration rim around xenocryst																		
13	9.1	0.03	553	12	0.02	185	2120	22	2121	14	0	0.1317	0.8	7.071	1.4	0.3894	1.2	0.832
14	4.1	0.31	420	52	0.13	143	2144	22	2133	16	–1	0.1326	0.9	7.213	1.5	0.3945	1.2	0.800
15	11.1	0.00	437	2	0.00	143	2079	21	2114	11	2	0.1312	0.6	6.884	1.3	0.3805	1.2	0.889
16	7.1	0.00	478	13	0.03	152	2029	21	2094	9	3	0.1297	0.5	6.616	1.3	0.3699	1.2	0.916
17	1.1	0.04	351	6	0.02	111	2013	21	2098	11	4	0.1300	0.6	6.572	1.3	0.3666	1.2	0.888
18	7.2	1.17	475	32	0.07	145	1937	20	2093	22	8	0.1296	1.3	6.264	1.8	0.3505	1.2	0.696
19	8.1	0.04	573	2	0.00	156	1772	18	2074	10	17	0.1282	0.6	5.593	1.3	0.3163	1.2	0.903
Xenocrysts-1 with disturbed U–Pb isotope system																		
20	2.1	0.00	91	52	0.59	31	2141	25	2146	20	0	0.1336	1.1	7.260	1.8	0.3940	1.3	0.762
21	5.1	0.16	85	69	0.84	28	2124	25	2132	22	0	0.1325	1.3	7.133	1.9	0.3903	1.4	0.728
22	10.1	–	229	62	0.28	78	2163	23	2172	13	0	0.1356	0.8	7.455	1.4	0.3988	1.2	0.853
23	12.1	–	61	51	0.87	21	2142	24	2152	18	0	0.1341	1.0	7.287	1.7	0.3942	1.3	0.791
24	14.1	–	138	38	0.29	45	2094	23	2109	17	1	0.1309	1.0	6.925	1.6	0.3838	1.3	0.797
25	9.2	0.07	325	316	1.01	109	2119	22	2135	13	1	0.1327	0.7	7.123	1.4	0.3892	1.2	0.854
26	4.2	–	608	370	0.63	207	2147	22	2175	8	1	0.1358	0.5	7.400	1.3	0.3951	1.2	0.932
Xenocrysts-1 with disturbed U–Pb isotope system																		
27	8.2	0.01	356	176	0.51	111	2003	21	2087	11	4	0.1292	0.6	6.491	1.4	0.3644	1.2	0.881
28	1.2	0.28	346	250	0.74	107	1975	21	2118	14	7	0.1315	0.8	6.503	1.4	0.3586	1.2	0.847
Xenocrysts-2 with disturbed U–Pb isotope system																		
29	3.1	0.04	162	125	0.80	56	2194	23	2202	15	0	0.1380	0.9	7.715	1.5	0.4055	1.3	0.821

Pb_c and Pb*—nonradiogenic and radiogenic elements respectively; (1)—correciton for P_c on measured ^{204}Pb; *D*, %—discordance $100 \times \{(^{207}Pb/^{206}Pb\ age)/(^{206}Pb/^{238}U\ age) - 1\}$; errors for interval ±σ; standard calibration errors are 0.39% (analyses 1–11) and 0.42% (analyses 12–29).
Analyses were performed on SHRIMP at the Center for Isotopic Research of the Karpinskii All-Russia Geological Research Institute (VSEGEI), analyst A.N. Larionov.

nation with host rocks, and subsequent hydrothermal metasomatic reworking of the dike rocks with formation of a wide range of SiO_2-saturated and oversaturated syenites and their K and ultra-K varieties. Isotope data on the assimilated xenocrysts of detrital zircon indicate that the host metaterrigenous rocks of the Vorontsovska Group were derived from a Paleoproterozoic (2200 ± 26 and 2143 ± 14 Ma) provenance.

REFERENCES

1. A. A. Arzamastsev, Zh. A. Fedotov, and L. V. Arzamastseva, *Dike Magmatism of the Northwestern Baltic Shield* (Nauka, St. Petersburg, 2009) [in Russian].
2. I. N. Bykov, *Upper Devonian Basalts of the Southeastern Voronezh Anteclise* (Voronezh, Gos. Univ., Voronezh, 1975) [in Russian].
3. M. M. Kalinkin, A. A. Arzamastsev, and I. V. Polyakov, Petrologiya **1** (2), 205–214 (1993).
4. U. Kramm, L. N. Kogarko, and V. A. Kononova, in *Magmatism of Rift and Fold Belts* (Nauka, Moscow, 1993), pp. 148–168 [in Russian].
5. V. M. Moralev, M. M. Arakelyants, A. S. Baluev, et al., Dokl. Earth Sci. **361A** (6), 786–789 (1998).
6. V. Yu. Skryabin and R. A. Terentiev, in *Trace Metals: Mineral—Raw Base, Development, Production, and Consumption. Proceedings of All-Russian Scientific—Practical Conference, Moscow, Russia, 2011* (IMGRE, Moscow, 2011), pp. 154–155 [in Russian].
7. V. S. Shchukin, S. M. Sablukov, L. I. Sablukova, et al., in *Deep Magmatism, Magmatic Sources, and Problems of Plumes. Proceedings of 2nd International Conference, Irkutsk, Russia, 2002* (Irkuts. Gos. Univ., Irkutsk, 2002), pp. 151–165 [in Russian].
8. W. Compston, M. S. Sambridge, R. T. Reinfrank, et al., J. Geol. Soc. London **152**, 599–610 (1995).
9. M. W. Martin, D. V. Grazhdankin, S. A. Bowring, et al., Science **288**, 841–845 (2000).
10. D. Roberts, Norg. Geol. Unders. **322**, 55–72 (1975).

Translated by M. Bogina